Angewandte Chemie
Eine Zeitschrift der Gesellschaft Deutscher Chemiker

Supporting Information

69451 Weinheim, Germany

Cyclopentadienylchromium complexes of 1,2,3,5-dithiadiazolyls: η^2 π-complexes of cyclic sulphur-nitrogen compounds**

Hiu Fung Lau, Victor Wee Lin Ng, Lip Lin Koh, Geok Kheng Tan, Lai Yoong Goh, Tracey L. Roemmele, Sonja D. Seagrave and René T. Boeré**

[*] Hiu Fung Lau, Victor Wee Lin Ng, Lip Lin Koh, Geok Kheng Tan and Dr. L.Y. Goh
Department of Chemistry
National University of Singapore
Kent Ridge (Singapore) 119260
Fax: (+65) 6779 1691
E-mail: chmgohly@nus.edu.sg

Prof. René T. Boeré, Tracey L. Roemmele, Sonja D. Seagrave
Department of Chemistry and Biochemistry
University of Lethbridge
Lethbridge, AB, T1K 3M4 (Canada)
Fax: +1-403-329-2057
Email: boere@uleth.ca

Supplementary material

(11 pages)

Experimental Details

All manipulations were carried out either under a nitrogen atmosphere using standard Schlenk techniques or under an argon atmosphere in a glove box. $[CpCr(CO)_3]_2$ (**2**) was prepared according to literature procedures from chromium hexacarbonyl (98% purity from Fluka).[1] **1c** was prepared by typical methods for dithiadiazolyls, and characterized by single-crystal X-ray diffraction (See below).

Preliminary NMR-scale reactions of **2** with **1a-c** were conducted at ambient temperature in toluene. It was observed that as the Cp resonance of **2** diminished, new Cp resonances appeared e.g. at δ 3.86, 4.36 and 4.91 which peaked in intensity after 1-2 h, at which time **2** was totally reacted and the solutions were reddish-brown. Trial chromatography showed that separation of the products was feasible on silica gel and neutral alumina columns. In the larger scale workup, described below, exhaustive chromatography on silica gel was employed.

$CpCr(CO)_2(\eta^2\text{-}S_2N_2CC_6H_4Me)$ (**3a**): $(4\text{-}Me\text{-}C_6H_4CN_2S_2)_2$ (**1a**) (97 mg, 0.25 mmol) and $[CpCr(CO)_3]_2$ (**2**) (100 mg, 0.25 mmol) were dissolved in toluene (7 mL) and stirred at ambient temperature for 2 h. The resultant reddish-brown reaction mixture was concentrated to dryness and subsequently extracted with n-hexane (10 x 1.5 mL), leaving behind on the walls of the flask a black solid (*ca*. 13 mg, 0.019 mmol, 7.6% yield by weight based on total reactants), which as yet could not be characterized. The reddish-brown extracts were filtered, concentrated to *ca*. 2 mL and loaded onto a silica gel column (2.0 x 10 cm) prepared in n-hexane. Elution gave 3 fractions: (i) a green eluate in n-hexane/toluene (3:2, 25 ml), which on concentration gave deep green crystals of $[CpCr(CO)_2]_2S$ (**4**) (*ca.* 13 mg, 0.034 mmol, 14% yield), identified by its colour and spectral characteristics (^{1}H NMR: δ(Cp) 4.36 in benzene-d_6 and FAB$^+$-MS: m/z 378.)[26] (ii) a red eluate in n-hexane/toluene (1:1, 15 ml), which yielded a red solid of **1a** (*ca.* 21 mg, 0.054

mmol, 22% recovery) identified by its EI^+-MS peak at m/z 195 (4-Me-$C_6H_4CN_2S_2$) and its fragmentation pattern. (iii) a red eluate in toluene (30 mL), which yielded a fine red crystalline solid of **3a** (*ca*. 80 mg, 0.22 mmol, 44% yield). An immovable green band (*ca*. 2 mm thick) was left uneluted on the column. Anal. for **3a**. Found: C, 48.9; H, 3.2; N, 8.0; S, 17.1. Calc. for $CpCr(CO)_2(S_2N_2CC_6H_4Me)$: C, 48.9; H, 3.3; N, 7.6; S, 17.4%. ^{1}H NMR (300MHz, 300 K, C_6D_6): δ(Cp) 3.86 (s, 5H); δ(C_6H_4) 8.14 (br, 26 Hz, 2H) and 6.94 (m, 2H); δ(CH_3) 2.00 (s, 3H). ^{13}C NMR (300MHz, 300 K, C_6D_6): δ(CH_3) 21.88; δ(Cp) 91.74 (br); δ(C_{meta}) 130.14; δ(C_{para}) 141.99; remaining ring C obscured by solvent; carbonyls not detected.) Solutions of these complexes have a rather low molar concentration of NMR-active nuclei, and the ^{13}C NMR are also affected by the dynamic processes from the *endo*/*exo* interconversion at room temperature. Thus full characterization of low-abundance nuclei NMR spectra was not possible for these derivatives. IR (KBr, cm^{-1}): ν(C=O) 1959vs and 1890vs. FAB^+-MS: m/z 369 $[M+1]^+$, 312 $[M-2CO]^+$, 266 $[M-2CO-SN]^+$, 195 $[CpCrS_2N]^+$.

$CpCr(CO)_2(\eta^2$-$S_2N_2CC_6H_4Cl)$ (**3b**): A similar procedure using **1b** (102 mg, 0.24 mmol) and **2** (96 mg, 0.24 mmol) gave **3b** (*ca*. 90 mg, 0.23 mmol, 48% yield) together with **4** (*ca*. 26 mg, 0.069 mmol, 29% yield). Anal. for **3b**. Found: C, 43.8; H, 2.8; N, 7.4; S, 17.1. Calc. for $CpCr(CO)_2(S_2N_2CC_6H_4Cl)$: C, 43.3; H, 2.3; N, 7.2; S, 16.5%. ^{1}H NMR (300MHz, 300 K, C_6D_6): δ(Cp) 3.80 (s, 5H); δ(C_6H_4) 7.89 (br, 37 Hz, 2H) and 7.02 (m, 2H). ^{13}C NMR (500MHz, 300 K, $C_6D_5CD_3$): δ(Cp) 88.7, 91.2; δ(CO) 248; ring carbons obscured by solvent. IR (KBr, cm^{-1}): ν(C=O) 1954vs and 1894vs. FAB^+-MS: m/z 389 ($[M+1]^+$ for ^{35}Cl), 332 $[M-2CO]^+$, 195 $[CpCrS_2N]^+$.

$CpCr(CO)_2(\eta^2\text{-}S_2N_2CC_6H_3\text{-}3\text{-}(CN)\text{-}5\text{-}(^tBu))$ (**3c**): Likewise the reaction of **1c** (132 mg, 0.25 mmol) with **2** (101 mg, 0.25 mmol), led to the isolation of **3c** (*ca*. 113 mg, 0.26 mmol, 52% yield) and **4** (*ca.* 23 mg, 0.06 mmol, 24% yield). Anal. for **3c**. Found: C, 52.0; H, 3.5; N, 9.5; S, 14.3. Calc. for $CpCr(CO)_2(S_2N_2CC_6H_3\text{-}3\text{-}(CN)\text{-}5\text{-}(^tBu))$: C, 52.4; H, 3.9; N, 9.7; S, 14.7%. ^{1}H NMR (300MHz, 300 K, C_6D_6): δ(Cp) 3.78 (s, 5H); δ(C_6H_3) 8.36 (br, 24 Hz, 1H) 8.16 (br, 24 Hz, 1H) and 7.36 (s, 1H); δ(CH_3) 0.96 (s, 9H). IR (KBr, cm^{-1}): ν(C=O) 1959vs and 1897vs. FAB^+-MS: m/z 436 $[M+1]^+$, 379 $[M\text{-}2CO]^+$, 195 $[CpCrS_2N]^+$. ^{13}C NMR not obtained (see **3a**,**b**).

Crystallographic Details

The crystals were mounted on quartz fibres. X-ray data were collected on a Siemens SMART diffractometer, equipped with a CCD Area Detector, using Mo Kα radiation (λ = 0.710 73 Å). The data were corrected for Lorentz and polarization effects with the SMART suite of programs and for adsorption effects with SADABS. Structure solution and refinement were carried out with the SHELXTL suite of programs. The structure was solved by direct methods to locate the heavy atoms, followed by difference maps for the light, non-hydrogen atoms. The Cp, aryl and alkyl hydrogen atoms were placed in calculated position.

3a: $C_{15}H_{12}CrN_2O_2S_2$, M_r = 368.39, triclinic, space group *P*-1, *a* = 7.7225(9), *b* = 9.7779(11), *c* = 11.7171(13) Å, α = 67.524(2), β = 86.123(2), γ = 69.230(2), *V* = 762.05(15) Å^3, *Z* = 2, ρ_{calcd} = 1.605 g cm^{-3}, μ = 1.031 mm^{-1}, *F*(000) = 376, *T* = 223(2) K. A dark red needle crystal (0.18 × 0.18 × 0.10 mm^3) was mounted on a glass fibre. Of the 10 001 reflections collected, 3489 were unique (R_{int} = 0.034) and used to refine 200 parameters. Refinement was carried out on F^2 against all independent reflections and converged at R_1 = 0.0511 [$I > 2\sigma(I)$] and wR_2 = 0.1139 (for all data).

3b: $C_{14}H_9CrClN_2O_2S_2$, M_r = 388.80, orthorhombic, space group *P*bca, a = 13.894(2), b = 10.9981(15), c = 19.653(3) Å, V = 3003.1(7) Å^3, Z = 8, ρ_{calcd} = 1.720 g cm^{-3}, μ = 1.223 mm^{-1}, F(000) = 1568, T = 223(2) K. A dark red plate crystal (0.28 × 0.22 × 0.03 mm^3) was mounted on a glass fiber. Of the 19 853 reflections collected, 3441 were unique (R_{int} = 0.066) and used to refine 199 parameters. Refinement was carried out on F^2 against all independent reflections and converged at R_1 = 0.0726 [$I > 2\sigma(I)$] and wR_2 = 0.1490 (for all data).

3c: $C_{19}H_{17}CrN_3O_2S_2$, M_r = 435.48, triclinic, space group *P*-1, a = 6.3689(15), b = 12.436(3), c = 12.857(3) Å, α = 106.480(5), β = 91.552(4), γ = 92.249(4), V = 974.9(4) Å^3, Z = 2, ρ_{calcd} = 1.483 g cm^{-3}, μ = 0.820 mm^{-1}, F(000) = 448, T = 295(2) K. A red plate crystal (0.19 × 0.10 × 0.04 mm^3) was mounted on a glass fibre. Of the 5146 reflections collected, 3418 were unique (R_{int} = 0.048) and used to refine 259 parameters with 18 restraints. The ^{t}Bu group was found to be disordered into two positions at 60/40 occupancy ratio. Refinement was carried out on F^2 against all independent reflections and converged at R_1 = 0.0703 [$I > 2\sigma(I)$] and wR_2 = 0.1690 (for all data).

1c: $C_{12}H_{12}N_3S_2$, M_r = 262.37, orthorhombic, space group *P*bca, a = 13.301(3), b = 10.5014(19), c = 18.530(4) Å, V = 2588.4(8) Å^3, Z = 8, ρ_{calcd} = 1.347 g cm^{-3}, μ = 0.392 mm^{-1}, F(000) = 1096, T = 223(2) K. A black block crystal (0.46 × 0.30 × 0.26 mm^3) was mounted on a glass fibre. Of the 16432 reflections collected, 2954 were unique (R_{int} = 0.034) and used to refine 181 parameters with 42 restraints. The ^{t}Bu group was found to be disordered into two positions at 50/50 occupancy ratio. Refinement was carried out on F^2 against all independent reflections and converged at R_1 = 0.0893 [$I > 2\sigma(I)$] and wR_2 = 0.2319 (for all data).

Preliminary Voltammetric Results and EPR Spectrum

Cyclic voltammograms of **3a** demonstrate an irreversible oxidation at potentials of +0.58 V vs. SCE, and a quasi-reversible reduction at –0.91 V vs. SCE. In an *in-situ* electrochemical reduction at a gold micromesh working electrode, a five-line EPR spectrum is obtained consistent with hyper-fine coupling to two equivalent ^{14}N nuclei, and with no evidence of coupling to chromium (Figure S1). The observed hyperfine coupling (hfc) constants of 0.594 mT, sharp lines and short lifetimes (first-order decay with $t_{1/2}$ = 5.7 sec) suggest that this reduction product is not a free dithiadiazolyl radical. The absence of chromium hfc is consistent with the DFT calculations which confirm that the LUMO of the complexes are heavily localized on the S_2N_2CR rings. Both the hfc and the narrow lines are different from those measured from solutions of **1a**.

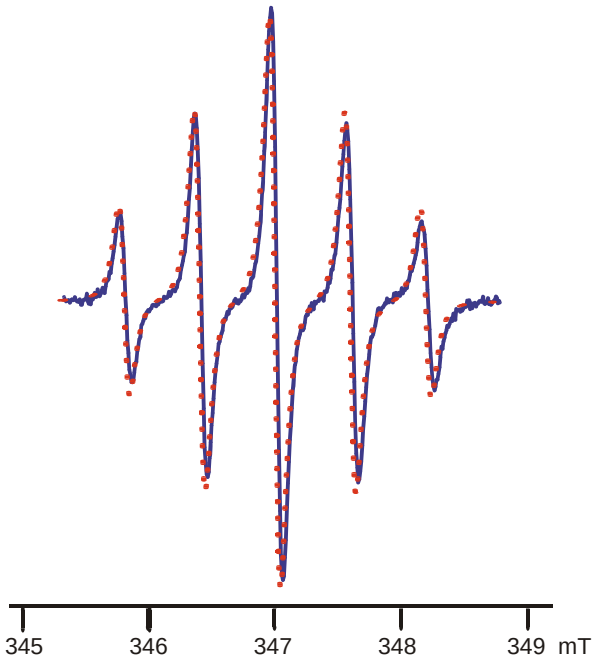

Figure S1 Experimental (blue line) and simulated (orange dots) EPR spectra obtained at a gold micromesh electrode upon reduction of **3a** (parameters from the simulation: hfc = 0.596 mT from two equivalent ^{14}N; lineshape = Lorentzian; linewidth = 0.08 mT). The *g* value is 2.00893.

B3PW91/6-31G+(d) Computed Structures of Model *exo* and *endo* $CpCr(CO)_2\{S_2N_2CH\}$ Complexes

The structures of diamagnetic adducts $\{\eta^5\text{–Cp}\}Cr(CO)_2\{\eta^2\text{–}S_2N_2CH\}$ were optimized with C_s symmetry in their ground states using density functional theory in the GAUSSIAN 98W suite of programs.[2] The B3PW91 functional[3] with the 1991 gradient-corrected correlation functional of Perdew and Wang[4] was used; this hybrid functional has previously been shown to provide realistic geometries for organochromium complexes.[5] The Gaussian basis set 6-31+G(d) was used for geometry optimization and 6-311+G(2d,2p) for the final energy calculations.

Exo isomer (-2409.1423602 Hartree):

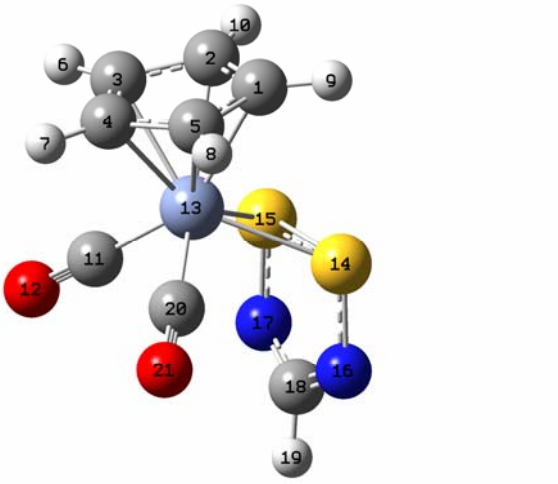

Distances, Å		Angles, °	
Cr—S14	2.37207	Cr—S14—N16	112.99488
Cr—C11	1.84126	Cr—S14—S16	62.2244
Cr—C1	2.22851	S15—S14—N16	92.63249
Cr—C4	2.14886	S14—N16—C18	114.23057
Cr—C5	2.17596	N16—C18—N17	125.23303
S14—S15	2.21081	S15—Cr—C11	84.56538
S14—N16	1.64776	C11—Cr—C20	81.87248
N16—C18	1.33013	S14—Cr—C1	85.02349
C11—O12	1.15827	S14—Cr—C5	105.5517
C1—C2	1.41912	S14—Cr—C4	143.97551
C1—C5	1.42011	C2—C1—C5	108.19446
C5—C4	1.42742	C1—C5—C4	107.92887
		C5—C4—C3	107.75051

Endo isomer (-2409.143318 Hartree):

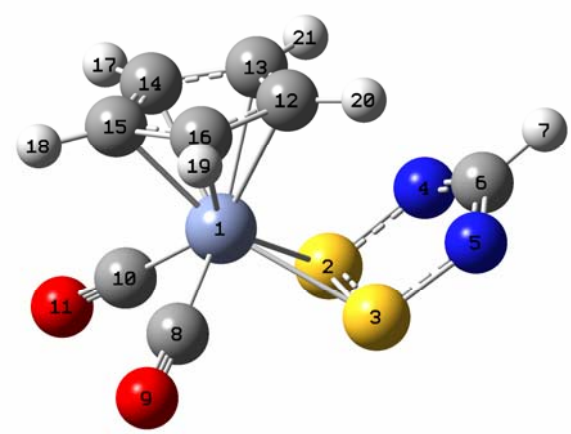

Distances, Å		Angles, °	
Cr—S2	2.3878	Cr—S2—N4	112.80999
Cr—C8	1.83815	Cr—S2—S3	62.47819
Cr—C12	2.22066	S3—S2—N4	92.76847
Cr—C15	2.15279	S2—N4—C6	114.22321
Cr—C16	2.17846	N4—C6—N5	125.38998
S2—S3	2.20210	S2—Cr—C10	81.37219
S2—N4	1.65417	C8—Cr—C10	81.66016
N4—C6	1.32903	S2—Cr—C13	90.70312
C8—O9	1.15954	S2—Cr—C14	109.48207
C12—C13	1.41806	S2—Cr—C15	147.94706
C12—C16	1.41959	C12—C13—C14	108.21153
C15—C16	1.42750	C13—C14—C15	107.93714
		C14—C15—C16	107.70257

The **endo** isomer is more stable by 2.51 kJ/mol

Bonding Analysis and Comparison to Allyl Complexes

The calculations also provide insights into the formal resemblance to the very recently reported $CpCr(CO)_2[R_2CC(R)CR_2]$ π-allyl complexes.[6] Strengthening this analogy is the fact that these Cr π-allyl complexes are also known to form both *exo* and *endo* isomers.

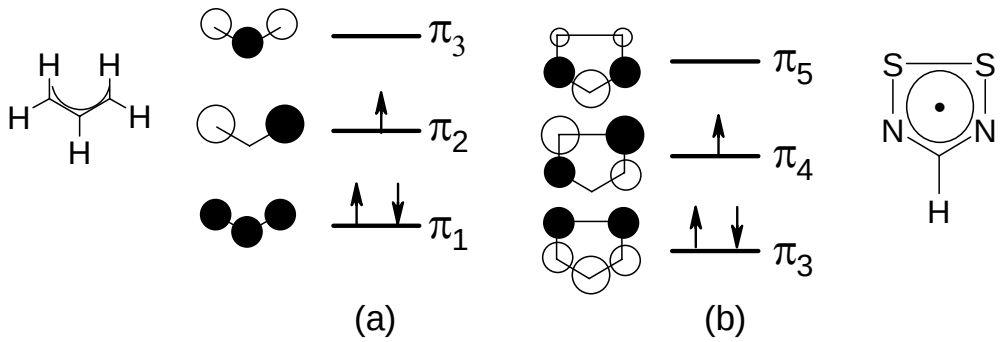

Scheme

Consideration of the frontier orbitals of (a) the allyl radical and (b) those of HCN_2S_2 (Scheme) emphasizes the similarity between the two systems. Topologically π_4 of the dithiadiazolyl resembles allyl π_2, while π_3 of the heterocyle resembles allyl π_1. The separation between the terminal C atoms of the allyl at ~2.4 Å is only a little larger than the ~2.1 Å between the two sulphur atoms of the dithiadiazolyl, and the *p* orbitals of the latter are expected to have larger effective radii, further minimizing the differences in ligand size. Energetically these two pairs of orbitals are also similar, while the lower π orbitals of the heterocyle are of no consequence in metal binding due to the high effective electronegativity of both nitrogen and sulphur.[7]

Fragment Interaction diagram

The major interactions between the orbitals $Cp(CO)_2Cr$ and S_2N_2CH radical fragments occur between the SOMO of the metal and the ring SOMO (π4) as well as between one other empty metal orbital and ring π3. The interactions are indicated along with orbital surface diagrams in the following diagram. The complex has the typical "t_{2g}" like set of three filled *d* orbitals.

Interaction diagram for $Cp(CO)_2CrS_2N_2CH$ model compound
(at calculated geometry)

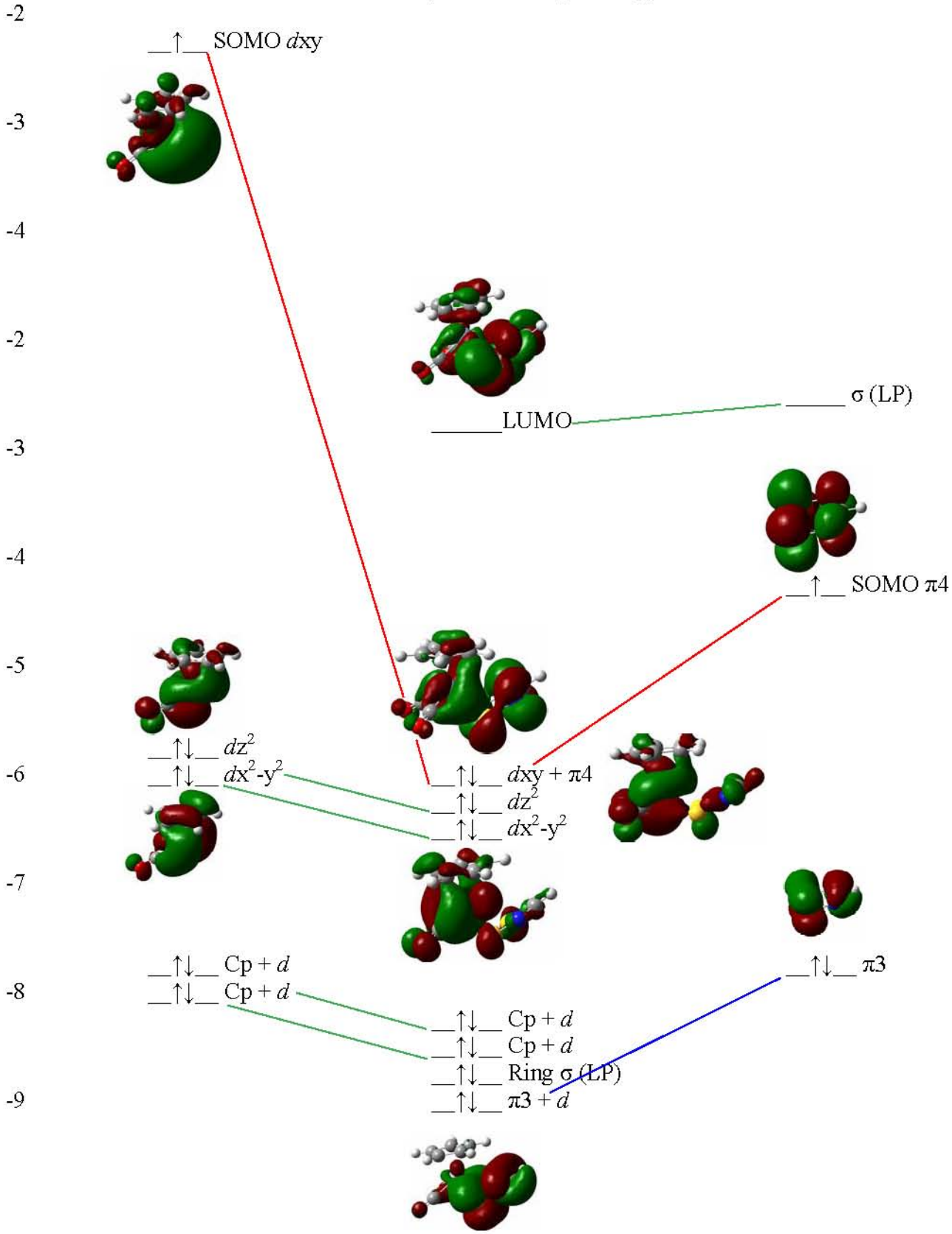

Only the main interacting fragments have been highlighted in this schematic representation.

References

[1] A. R. Manning, P. Hackett, R. Birdwhistell, P. Soye, *Inorg. Synth.* **1990**, *28*, 148.

[2] Gaussian 98W, Revision A.9, M. J. Frisch, *et al.* Gaussian, Inc., Pittsburg, PA, 1998.

[3] A. D. Becke, *J. Chem. Phys*. **1993**, *98*, 5648.

[4] J. P. Perdew, Y. Wang, *Phys. Rev. B* **1992**, *45*, 13244.

[5] C. N. Carlson, J. D. Smith, T. P. Hanusa, W. W. Brennessel, V. G. Young, Jr., *J. Organomet. Chem.* **2003**, *683*, 191.

[6] D. W. Norman, M. J. Ferguson, J. M. Stryker, *Organometallics* **2004**, *23*, 2015.

[7] R. T. Oakley, *Prog. Inorg. Chem.* **1988**, *36*, 299.